

Platinum Indolylphosphine Fluorido and Polyfluorido Complexes: An Interplay between Cyclometallation, Fluoride Migration, and Hydrogen Bonding

Stefan Sander,^[a] Robert Müller,^[b] Mike Ahrens,^[a] Martin Kaupp,^{*,[b]} and Thomas Braun^{*,[a]}

Abstract: The reaction of [PtCl₂(COD)] (COD = 1,5-cyclooctadiene) with diisopropyl-2-(3-methyl)indolylphosphine (*i*Pr₂P(C₉H₈N)) led to the formation of the platinum(II) chlorido complexes, *cis*-[PtCl₂{*i*Pr₂P(C₉H₈N)}₂] (1) and *trans*-[PtCl₂{*i*Pr₂P(C₉H₈N)}₂] (2). The *cis*-complex 1 reacted with NEt₃ yielding the complex *cis*-[PtCl{κ²-(*P,N*)-*i*Pr₂P(C₉H₇N)}{*i*Pr₂P(C₉H₈N)}] (3) bearing a cyclometalated κ²-(*P,N*)-phosphine ligand, while the isomer 2 with a *trans*-configuration did not show any reactivity towards NEt₃. Treatment of 1 or 3 with (CH₃)₄NF (TMAF) resulted in the formation of the twofold cyclometalated complex *cis*-[Pt{κ²-(*P,N*)-*i*Pr₂P(C₉H₇N)}₂] (4). The molecular structures of the complexes 1–4 were determined by single-crystal X-ray diffraction. The fluorido complex *cis*-[PtF{κ²-(*P,N*)-*i*Pr₂P(C₉H₇N)}{*i*Pr₂P(C₉H₈N)}]·(HF)₄ (5·(HF)₄) was

formed when complex 4 was treated with different hydrogen fluoride sources. The Pt(II) fluorido complex 5·(HF)₄ exhibits intramolecular hydrogen bonding in its outer coordination sphere between the fluorido ligand and the NH group of the 3-methylindolyl moiety. In contrast to its chlorido analogue 3, complex 5·(HF)₄ reacted with CO or the ynamide 1-(2-phenylethynyl)-2-pyrrolidinone to yield the complexes *trans*-[Pt(CO){κ²-(*P,C*)-*i*Pr₂P(C₉H₇NCO)}{*i*Pr₂P(C₉H₈N)}][F(HF)₄] (7) and a complex, which we suggest to be *cis*-[Pt{C=C(Ph)OCN(C₃H₆)}{κ²-(*P,N*)-*i*Pr₂P(C₉H₇N)}{*i*Pr₂P(C₉H₈N)}][F(HF)₄] (9), respectively. The structure of 9 was assigned on the basis of DFT calculations as well as NMR and IR data. Hydrogen bonding of HF and NH to fluoride was proven to be crucial for the existence of 7 and 9.

Introduction

Fluorido complexes of late transition metals gain increasing attention,^[1] in part because of their ability to open up original routes for metal-mediated fluorination reactions.^[1h,i,2] In addition, they can also play a distinct role in C–F or C–H activation reactions.^[1j,n,3] However, late transition metal fluorido complexes tend to be unstable, which is often explained by the mismatch of a soft Lewis acid with a hard Lewis base, but also with an unfavourable p(π)-d(π) repulsion.^[4] The first examples of platinum(II) fluorido complexes were already described in the early 1970s.^[1a,5] Platinum fluorido complexes came again into focus in recent years.^[1d,e,6] Wendt et al., Vigalok et al. and recently Beyzavi, Shahsavari et al. described the preparation of

Pt(II) fluorido complexes by a F/I exchange reaction with AgF.^[1d,e,6i] Platinum fluorido complexes were also obtained by reaction of hydrogen fluoride sources with platinum hydrido or dimethyl complexes, as shown by Perutz et al. and Seppelt et al., respectively.^[6a,g] Braun et al. revealed that Pt alkyne complexes react with N-Fluorobenzenesulfonimide (NFSI) or XeF₂ to give platinum fluorido and β-fluorovinyl complexes.^[6h,j] Vigalok et al., Puddephatt et al. and Haghghi et al. reported on the formation of Pt(IV) fluorido complexes using XeF₂, NFSI or Selectfluor (*N*-chloromethyl-*N'*-fluorotriethylenediammonium bis(tetrafluoroborate)).^[6d,i,m] Love et al. demonstrated Pt(II) mediated C–F bond activation reactions generating Pt(IV) fluorido complexes,^[6b,c,e,f] while Finze, Braunschweig and Bickelhaupt et al. presented the formation of a trifluorophosphane platinum (II) fluorido complex by P–F bond activation of PF₅.^[6k]

Hydrogen bonding is discussed as an important factor to enable fluorination reactions by increasing the *effective nucleophilicity* of the fluoride, due to a lowering of its basicity.^[7] Richmond et al. reported on the potential of transition metal fluorido complexes to act as hydrogen bond acceptors.^[8] The ability of transition metal fluorido complexes to undergo strong hydrogen bonding with hydrogen fluoride to result in the formation of bifluorido complexes is well described.^[1m,6a,9] NH or OH groups were also employed as hydrogen bond donors for transition metal fluorides.^[1k,10] Thus, Crabtree et al. probed intramolecular hydrogen bonding of a ligand appended amino group to an Iridium(III) fluorido complex.^[10a,b] Gray et al. reported on a cyclometalated Iridium(III) fluorido complex exhibiting intramolecular hydrogen bonding to an adjacent pyrazole ligand.^[10e] Szymczak et al. demonstrated a remarkable

[a] S. Sander, Dr. M. Ahrens, Prof. Dr. T. Braun
Department of Chemistry
Humboldt-Universität zu Berlin
Brook-Taylor-Str. 2, 12489 Berlin (Germany)
E-mail: thomas.braun@cms.hu-berlin.de

[b] Dr. R. Müller, Prof. Dr. M. Kaupp
Institut für Chemie
Technische Universität Berlin, Theoretische Chemie/Quantenchemie, Sekr.C7
Straße des 17. Juni 135, 10623 Berlin (Germany)
E-mail: martin.kaupp@tu-berlin.de

Supporting information for this article is available on the WWW under <https://doi.org/10.1002/chem.202102451>

© 2021 The Authors. Chemistry - A European Journal published by Wiley-VCH GmbH. This is an open access article under the terms of the Creative Commons Attribution Non-Commercial NoDerivs License, which permits use and distribution in any medium, provided the original work is properly cited, the use is non-commercial and no modifications or adaptations are made.

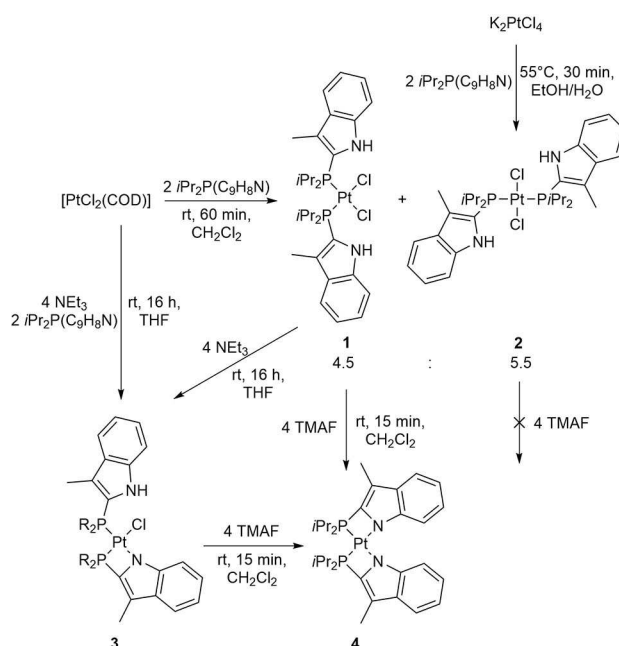
redox-induced Cu(II)-F bond dissociation to yield a copper(I) complex with a fluoride anion, which was then encapsulated in the secondary coordination sphere through hydrogen bonding with a tripodal ligand featuring three pendant OH-groups.^[109] Very recently, the same group presented a hydrogen-bonded Ni(I) and Ni(II) fluoro complex featuring a tris(2-pyridylmethyl) amine ligand.^[111] Nocera, Cummins and co-workers presented a Co(II) complex with a bicyclic cryptand bearing carboxamide NH-donors which turned out to be a powerful tool to identify fluoride anions colorimetrically.^[107] Perutz and Brammer et al. reported on interesting studies on the exceptionally strong hydrogen bond acceptor character of transition metal group 10 fluorides.^[110] They employed indole amongst other molecules and estimated the enthalpies and entropies of hydrogen-bonding interactions with early and late transition metal fluoro complexes. Parkin et al. also probed indole as an excellent hydrogen bond donor molecule for zinc and magnesium fluoro complexes.^[112] Farrar et al. reported first on the synthesis of 2-(3-methyl)indole substituted phosphine ligands and proved their high affinity towards fluoride anions.^[113] The coordination of 2-(3-methyl)indolyl phosphine ligands to various transition metal complexes was examined in recent years by the groups of Farrar et al., Koshevoy, Tunik et al. and Owen et al.^[13a,14] However, these studies are limited to chlorido complexes and the capability of 2-(3-methyl)indolylphosphine ligands to form hydrogen bonds to fluoro complexes has been unexploited, so far.

Herein, we report on the synthesis of platinum complexes bearing a diisopropyl-3-methyl-2-indolylphosphine ligand and their reactivity towards tetramethylammonium fluoride (TMAF) as well as hydrogen fluoride sources. A unique Pt(II) fluoro complex is described, which exhibits intramolecular hydrogen bonding to a fluoride in its coordination sphere. It shows a remarkable reactivity towards carbon monoxide and an ynamide, whereas its chlorido analogue did not react towards these substrates.

Results and Discussion

Synthesis of platinum(II) chlorido complexes with 3-methyl-2-indolylphosphine ligands

Treatment of $[\text{PtCl}_2(\text{COD})]$ with two equivalents of $i\text{Pr}_2\text{P}(\text{C}_9\text{H}_8\text{N})$ led to the formation of the platinum(II) complexes *cis*- $[\text{PtCl}_2\{i\text{Pr}_2\text{P}(\text{C}_9\text{H}_8\text{N})\}_2]$ (**1**) and *trans*- $[\text{PtCl}_2\{i\text{Pr}_2\text{P}(\text{C}_9\text{H}_8\text{N})\}_2]$ (**2**) in a ratio of 4.5 : 5.5 (Scheme 1). Complex **2** could be removed from the crude product mixture by washing the solid with a $\text{CH}_2\text{Cl}_2/n$ -hexane mixture (1:3), resulting in **1** as a colourless solid. The complex *trans*- $[\text{PtCl}_2\{i\text{Pr}_2\text{P}(\text{C}_9\text{H}_8\text{N})\}_2]$ (**2**) was synthesised independently by reaction of K_2PtCl_4 with two equivalents of $i\text{Pr}_2\text{P}(\text{C}_9\text{H}_8\text{N})$ in EtOH/ H_2O , following a modified procedure for the formation of *trans*- $[\text{PtCl}_2(\text{P}i\text{Pr}_3)_2]$.^[15] When the complex *cis*- $[\text{PtCl}_2\{i\text{Pr}_2\text{P}(\text{C}_9\text{H}_8\text{N})\}_2]$ (**1**) was treated with an excess of NEt_3 , cyclometallation and the formation of *cis*- $[\text{PtCl}\{\kappa^2-(P,N)-i\text{Pr}_2\text{P}(\text{C}_9\text{H}_7\text{N})\}\{i\text{Pr}_2\text{P}(\text{C}_9\text{H}_8\text{N})\}]$ (**3**) was observed (Scheme 1). Complex **3** was also obtained directly by adding a solution of $i\text{Pr}_2\text{P}(\text{C}_9\text{H}_8\text{N})$



Scheme 1. Synthesis of the platinum(II) complexes 1–4.

together with NEt_3 to a suspension of $[\text{PtCl}_2(\text{COD})]$ in THF. However, complex **2** bearing the phosphines in a *trans* position did not show any reactivity towards NEt_3 . This might be because a chlorido ligand in the *trans* position to the phosphine is more labile than the one *trans* to a chlorido ligand.

All complexes were characterised by ^1H NMR and $^{31}\text{P}\{^1\text{H}\}$ NMR spectroscopy as well as IR-spectroscopy. A comparison of selected NMR and IR data is shown in Table 1. The $^{31}\text{P}\{^1\text{H}\}$ NMR spectra of the complexes **1** and **2** reveal a singlet with ^{195}Pt satellites for the phosphorus atoms of the phosphine ligands. The values of the $^1J(\text{P,Pt})$ coupling constants (3580 Hz for **1** and 2490 Hz for **2**) are consistent with the *cis* or *trans* arrangement of the phosphine ligands.^[16] The $^{31}\text{P}\{^1\text{H}\}$ NMR spectrum of **3**

Table 1. Selected NMR and IR data for the complexes 1–5, and 7–9.

compound	$^{31}\text{P}\{^1\text{H}\}$ NMR ^[a] δ [ppm]	$^1J(\text{P,Pt})$ [Hz]	^1H NMR ^[a] δ (NH) [ppm]	IR data $\tilde{\nu}$ (N–H) [cm^{-1}]
$i\text{Pr}_2\text{P}(\text{C}_9\text{H}_8\text{N})$	–18.5	–	8.00	3423
1	18.6	3580	8.22	3333, 3278
2	23.2	2490	8.46	3396
3	17.5, –7.8	3231, 3083	8.68	3413
4	–10.1	2781	–	–
5	19.0, –18.0	3348, 3208	10.64	–
5 ·(HF) ₄	19.6, –18.0	3311, 3081	9.18	3404
6	179.9, 7.0	3991, 1498	8.25	–
7	55.7, 31.8	2268, 2605	10.61	3350–3150 ^[b]
8	47.8	2868	–	–
9	11.6, 3.1	3112, 1892	10.22	3263
10	16.6, –18.5	3315, 3478	9.80	3245
11	11.4, –3.3	3130, 1893	10.79	3208

[a] All NMR data were recorded using CD_2Cl_2 as solvent. [b] NH absorption band appeared strongly broadened in the region between 3350–3150 cm^{-1} .

exhibits two doublets with ^{195}Pt satellites at $\delta = 17.5$ ppm ($^2J(\text{P},\text{P}) = 14.0$ Hz, $^1J(\text{P},\text{Pt}) = 3231$ Hz) and $\delta = -7.8$ ppm ($^2J(\text{P},\text{P}) = 14.0$ Hz, $^1J(\text{P},\text{Pt}) = 3083$ Hz). Note, that the signal of the $\kappa^2\text{-P},\text{N}$ bound phosphine ligand appears high field shifted. The $^2J(\text{P},\text{P})$ coupling constants are typical for platinum complexes bearing phosphine ligands in a mutually *cis* coordination.^[17] The ^1H NMR spectra of **1**, **2**, and **3** show each a broad signal for the NH group in a region of $\delta = 8.22\text{--}8.68$ ppm. The resonances of the NH protons show for all complexes a downfield shift compared to the data for the free phosphine, which is consistent with hydrogen bonding interactions to the chlorido ligands.^[13,14c] The IR spectrum of *cis*-[PtCl₂{iPr₂P(C₉H₈N)}₂] (**1**) reveals two characteristic N–H stretching frequencies at $\tilde{\nu}(\text{NH}) = 3333, 3278$ cm⁻¹. The ATR IR spectra of *trans*-[PtCl₂{iPr₂P(C₉H₈N)}₂] (**2**) and *cis*-[PtCl₂{ $\kappa^2\text{-}(P,\text{N})\text{-iPr}_2\text{P}(\text{C}_9\text{H}_7\text{N})\}$ {iPr₂P(C₉H₈N)}] (**3**) show only a single broad absorption band at $\tilde{\nu}(\text{NH}) = 3396$ cm⁻¹ and 3413 cm⁻¹, respectively. Comparison to the N–H absorption frequencies of the

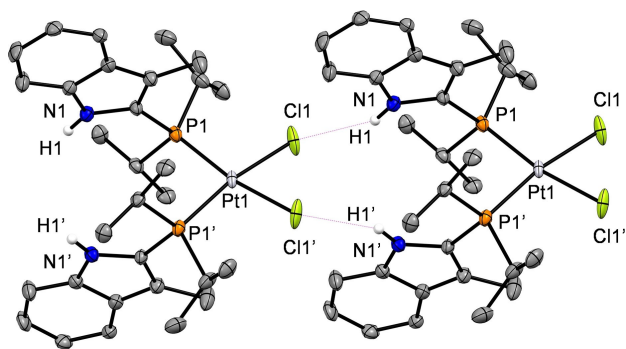


Figure 1. Extended structure of *cis*-[PtCl₂{iPr₂P(C₉H₈N)}₂] (**1**) revealing its intermolecular interactions. Thermal ellipsoids are drawn at 50% probability level, the intermolecular hydrogen bond is depicted as a magenta dashed line. Carbon bound hydrogen atoms and the solvent molecule were omitted for clarity. Selected bond lengths, distances [Å] and bond angles [°]: Pt1–P1 2.2890(9), Pt1–Cl1 2.3561(9), N1...Cl1 3.300(3), P1–Pt1–Cl1 90.99(3), P1–Pt1–P1 95.66(4), Cl1–Pt1–Cl1 83.21(5), N1–H1... Cl1 150(4).

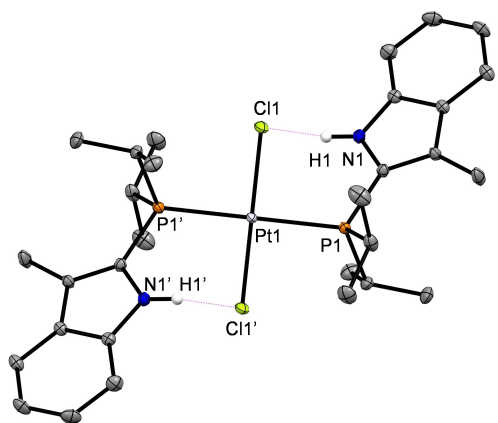


Figure 2. Molecular structure of *trans*-[PtCl₂{iPr₂P(C₉H₈N)}₂] (**2**). Thermal ellipsoids are drawn at 50% probability level, the intramolecular hydrogen bond is depicted as a magenta dashed line. Carbon bound hydrogen atoms and the solvent molecule were omitted for clarity. Selected bond lengths, distances [Å] and bond angles [°]: Pt1–P1 2.3428(7); Pt1–Cl1 2.3050(6); N1...Cl1 3.144(2); P1–Pt1–Cl1 90.46(2); N1–H1...Cl1 120(3).

phosphine iPr₂P(C₉H₈N) (3423 cm⁻¹) revealed shifts to lower frequencies together with broadened absorption bands, which is consistent for the presence of hydrogen bonding in solid state.^[18]

The molecular structures of the complexes *cis*-[PtCl₂{iPr₂P(C₉H₈N)}₂] (**1**), *trans*-[PtCl₂{iPr₂P(C₉H₈N)}₂] (**2**) and *cis*-[PtCl₂{ $\kappa^2\text{-}(P,\text{N})\text{-iPr}_2\text{P}(\text{C}_9\text{H}_7\text{N})\}$ {iPr₂P(C₉H₈N)}] (**3**) were obtained by X-ray crystallography, and they are depicted in the Figures 1–4. Selected bond lengths, angles and atomic distances are given in the captions of the corresponding Figures. Electron density for nitrogen bound hydrogen atoms were found in the difference Fourier maps and a free refinement was allowed. The molecular structures of **1** and **2** exhibit a slightly distorted square-planar coordination of the two $\kappa^1\text{-}(P)$ -phosphine and chlorido ligands in a mutually *cis* and *trans* coordination, respectively. For both structures, the asymmetric unit contains one half of the molecule. The Pt–P bond length of complex **1** (2.2890(9) Å) features a smaller value than the Pt–P bond length in complex **2** (2.3428(7) Å), while the opposite trend is seen for the Pt–Cl bond lengths (2.3561(9) Å for **1**, 2.3050(6) Å for **2**), resulting from the larger *trans*-influence of the phosphine ligands. The Pt–P and P–Cl bond lengths are in good

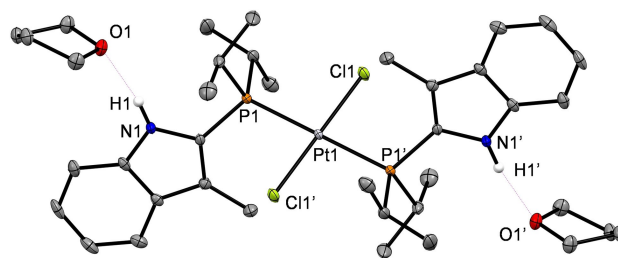


Figure 3. Molecular structure of *trans*-[PtCl₂{iPr₂P(C₉H₈N)}₂] · 2 C₄H₈O (2 · 2 C₄H₈O). Thermal ellipsoids are drawn at 50% probability level, the hydrogen bond to the solvent molecule is depicted as a magenta dashed line. Carbon bound hydrogen atoms were omitted for clarity. Selected bond lengths, distances [Å] and bond angles [°]: Pt1–P1 2.3192(5); Pt1–Cl1 2.33146(5); N1...O1 2.827(2); P1–Pt1–Cl1 90.010(18); N1–H1...Cl1 171(2).

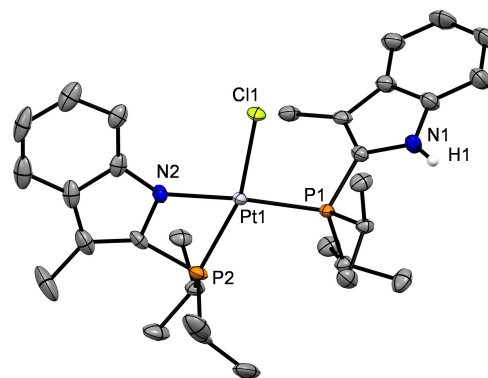


Figure 4. Molecular structure of *cis*-[PtCl₂{ $\kappa^2\text{-}(P,\text{N})\text{-iPr}_2\text{P}(\text{C}_9\text{H}_7\text{N})\}$ {iPr₂P(C₉H₈N)}] (**3**). Thermal ellipsoids are drawn at 50% probability level. Carbon bound hydrogen atoms and the solvent molecule were omitted for clarity. Selected bond lengths [Å] and bond angles [°]: Pt1–P1 2.2621(11); Pt1–P2 2.2868(13); Pt1–Cl1 2.3535(13); Pt1–N2 2.061(3); P1–Pt1–Cl1 90.72(3); P1–Pt1–P2 106.64(4); P2–Pt1–N2 69.07(9); Cl1–Pt1–N2 93.61(9).

accordance with data for similar dichlorido Pt(II) complexes bearing phosphine ligands in mutually *cis*- or *trans*-positions.^[19] It is well known, that chlorido ligands are good hydrogen bond acceptors.^[20] Thus, the N–H groups of the indolyl moieties are oriented in such a way, that hydrogen bonding to the chlorido ligands can be observed for **1** and **2**. Interestingly, complex **1** shows an intermolecular hydrogen bond motif in its extended molecular structure in the solid state, whereas intramolecular hydrogen bonding occurs in the structure of complex **2**. The N...Cl separations of **1** (3.300(3) Å) and **2** (3.144(2) Å) exhibit typical values for N–H...Cl hydrogen bond interactions.^[21] Recently, Owen et al. reported on the structures of two platinum chlorido complexes with diphenyl-2-(3-methylindolyl) phosphine ligands revealing intermolecular hydrogen bonding to the chlorido ligands in both cases.^[14e] However, the hydrogen bond to the chlorido ligands is easily broken when a stronger hydrogen bond acceptor like tetrahydrofuran (THF) is present, as it is shown in the molecular structure of **2**·2C₄H₈O (Figure 3). Note, that the Pt1–Cl1 bond gets elongated, while the Pt1–P1 bond is shortened when the intramolecular hydrogen bond is switched off by THF.

The molecular structure of complex *cis*-[PtCl{κ²-(*P,N*)-iPr₂P-(C₉H₇N)}]{iPr₂P(C₉H₈N)}] (**3**) shows a distorted square-planar coordination arrangement of the ligands at the platinum centre with one bidentate κ²-(*P,N*)-phosphine ligand forming a four membered metallacycle. The distortion is reflected by the small P2–Pt1–N2 bond angle of 69.07(9)°. Consequently, the P1–Pt1–P2 angle is increased to 106.64(4)°, while the P1–Pt1–Cl1 (90.72(3)°) and the Cl1–Pt1–N2 angles (93.61(9)°) differ only marginally from the ideal value of 90 degree. The P–Pt bond length of the phosphine bound in the *trans* position to the chlorido ligand (2.2868(13) Å) is comparable to the P–Pt bond lengths found in the molecular structures of its precursor complex **1**, while the P–Pt bond length of the phosphine located *trans* to the nitrogen atom is slightly shortened (2.2621(11) Å). Surprisingly, the molecular structure of **3** does not reveal hydrogen bonding from the N–H group to the chlorido ligand. However, in the expanded structure the NH group is oriented to another 3-methylindole moiety featuring a possible N–H...π hydrogen bond from the nitrogen to the calculated centroid of the six membered ring of the indole unit. An aromatic system is described as an excellent hydrogen bond acceptor,^[22] and several examples for N–H...π hydrogen bonds were described in the literature.^[23]

Reactivity of Pt chlorido complexes towards TMAF

Anhydrous tetramethylammonium fluoride (TMAF) is frequently used for nucleophilic fluorination reactions, because of its ability to deliver a rather nucleophilic fluoride.^[24] TMAF was also applied for the synthesis of several fluoro complexes starting from their halido precursors.^[10,25] Note that a highly nucleophilic fluoride can also act as a strong Lewis base to give for instance in the presence of HF the bifluoride anion.^[1f,26] However, when the complexes *cis*-[PtCl₂{iPr₂P(C₉H₈N)}₂] (**1**) or *cis*-[PtCl{κ²-(*P,N*)-iPr₂P(C₉H₇N)}]{iPr₂P(C₉H₈N)}] (**3**) were treated with an excess of

TMAF the formation of the complex *cis*-[Pt{κ²-(*P,N*)-iPr₂P-(C₉H₇N)}₂] (**4**) was observed (Scheme 1). The ¹⁹F NMR spectrum of the reaction mixture revealed the generation of the FHF[−] anion, which exhibits the characteristic doublet at δ = −151 ppm and a ¹J(F,H) coupling constant of 122 Hz.^[27] No reaction of *trans*-[PtCl₂{iPr₂P(C₉H₈N)}₂] (**2**) towards TMAF was observed.

Complex **4** could be separated from the tetramethylammonium salts by extraction of the crude product with toluene. The ³¹P{¹H} NMR spectrum of **4** exhibits a high field shifted singlet with ¹⁹⁵Pt satellites at δ = −10.1 ppm with a ¹J(P,Pt) coupling constant of 2784 Hz. The molecular structure of complex **4** in the solid state was determined by X-ray crystal structure determination (Figure 5). Complex **4** exhibits a distorted square-planar coordination geometry with two bidentate κ²-(*P,N*)-phosphine ligands in a mutually *cis* arrangement. The P(1)–Pt(1) and Pt(2)–P(2) bond lengths show almost the same values, which is also observed for the N(1)–Pt(1)/N(2)–Pt(1) bond lengths (2.2498(6) Å/2.2450(6) Å and 2.126(2) Å/2.128(2) Å, respectively). As a consequence of the two cyclometalated κ²-(*P,N*)-phosphine ligands, the P(1)–Pt(1)–N(1) and P(2)–Pt(1)–N(2) angles exhibit small values of 68.99(5)° and 69.39(5)°, respectively. Therefore, the P(1)–Pt(1)–P(2) (110.16(2)°), as well as the N(1)–Pt(1)–N(2) (111.52(7)°) bond angles are increased.

The formation of **4** from the (di-)chlorido platinum(II) precursors **1** or **3** with TMAF might proceed via two different pathways. One conceivable pathway involves an initial deprotonation of the 3-methylindole moiety of the phosphine ligand by fluoride followed by the cyclometallation and release of chloride. The second possible route consists of an Cl/F exchange at the Pt(II) centre and a subsequent HF elimination, which might again be supported by a fluoride base. For both steps FHF[−] would be formed, the signal of which was observed in the ¹⁹F NMR spectrum.

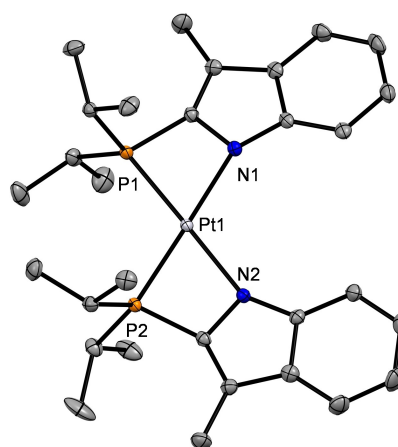
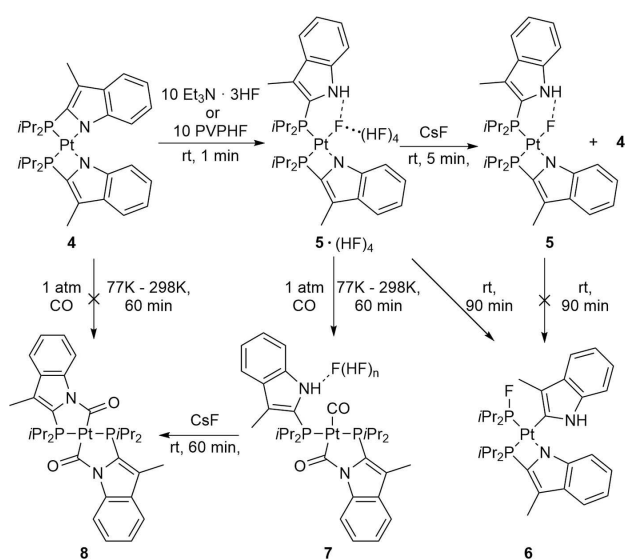


Figure 5. Structure of *cis*-[Pt{κ²-(*P,N*)-iPr₂P(C₉H₇N)}₂] (**4**). Thermal ellipsoids are drawn at 50% probability level. Hydrogen atoms were omitted for clarity. Selected distances (Å) and angles (°): Pt1–P1 2.2498(6); Pt1–P2 2.2450(6); Pt1–N1 2.126(2); Pt1–N2 2.128(2); P1–Pt1–P2 110.16(2); P1–Pt1–N1 68.99(5); P2–Pt1–N2 69.39(5); N1–Pt1–N2 111.52(7).

Reactivity of 4 towards hydrogen fluoride sources

To investigate a possible ring-opening at complex 4, the reactivity towards the HF sources $\text{Et}_3\text{N}\cdot 3\text{HF}$ or polymer supported poly[4-vinylpyridinium poly(hydrogen fluoride)] (PVPHF) was studied. After treatment of a solution of complex 4 with a ten-fold excess of the hydrogen fluoride sources, the formation of the Pt(II) fluoro complex $\text{cis}[\text{PtF}\{\kappa^2\text{-}(P,N)\text{-iPr}_2\text{P}(\text{C}_9\text{H}_7\text{N})\}\{\text{iPr}_2\text{P}(\text{C}_9\text{H}_8\text{N})\}]\cdot(\text{HF})_4$ ($5\cdot(\text{HF})_4$) was observed (Scheme 2). To determine the amount of pendant HF, a solution of complex $5\cdot(\text{HF})_4$ was treated with ten equivalents of Et_3SiCl . A full conversion to complex 1 as well as the formation of Et_3SiF was detected. The signal for Et_3SiF in the ^{19}F NMR spectrum was integrated towards an internal standard (C_6F_6) revealing values between 3.8 and 4.1 HF equivalents. The $^{31}\text{P}\{^1\text{H}\}$ NMR spectrum



Scheme 2. Formation of the Pt(II) fluoro complex $\text{cis}[\text{PtF}\{\kappa^2\text{-}(P,N)\text{-iPr}_2\text{P}(\text{C}_9\text{H}_7\text{N})\}\{\text{iPr}_2\text{P}(\text{C}_9\text{H}_8\text{N})\}]\cdot(\text{HF})_4$ ($5\cdot(\text{HF})_4$), its reactivity towards CsF, CO and the rearrangement reaction to the fluorophosphine complex $\text{cis}[\text{Pt}(\text{C}_9\text{H}_8\text{N})\{\kappa^2\text{-}(P,N)\text{-iPr}_2\text{P}(\text{C}_9\text{H}_7\text{N})\}\{\text{iPr}_2\text{PF}\}]$ (**6**).

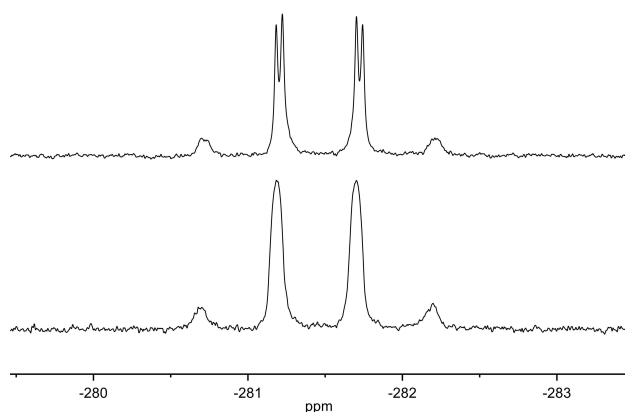


Figure 6. Part of the ^{19}F NMR spectrum (bottom) and the $^{19}\text{F}\{^1\text{H}\}$ NMR spectrum (top) of $\text{cis}[\text{PtF}\{\kappa^2\text{-}(P,N)\text{-iPr}_2\text{P}(\text{C}_9\text{H}_7\text{N})\}\{\text{iPr}_2\text{P}(\text{C}_9\text{H}_8\text{N})\}]\cdot(\text{HF})_4$ ($5\cdot(\text{HF})_4$) revealing coupling constants of $^2J(\text{F},\text{P}) = 146.8$ Hz, $^2J(\text{F},\text{P}) = 11.3$ Hz, $^1J(\text{F},\text{Pt}) = 283$ Hz. Note that part of the ^{195}Pt satellites is hidden by the main signal.

of the fluoro complex $5\cdot(\text{HF})_4$ exhibits two signals for the two different phosphine ligands. The resonance at $\delta = 19.6$ ppm displays as a doublet of doublets with ^{195}Pt satellites with coupling constants of $^2J(\text{P},\text{P}) = 16.5$ Hz, $^2J(\text{P},\text{F}) = 11.3$ Hz and $^1J(\text{P},\text{Pt}) = 3311$ Hz and can be assigned to the phosphorus atom in the *cis* position to the fluoro ligand. The doublet of doublets with ^{195}Pt satellites at -18.0 ppm, exhibiting coupling constants of $^2J(\text{P},\text{P}) = 16.5$ Hz, $^2J(\text{P},\text{F}) = 146.8$ Hz and $^1J(\text{P},\text{Pt}) = 3081$ Hz is allocated to the phosphorus atom *trans* to the fluoro ligand. The $^{19}\text{F}\{^1\text{H}\}$ NMR spectrum revealed a doublet of doublets with ^{195}Pt satellites at $\delta = -281.5$ ppm with coupling constants of $^2J(\text{F},\text{P}) = 146.8$ Hz, $^2J(\text{F},\text{P}) = 11.3$ Hz and $^1J(\text{F},\text{Pt}) = 283$ Hz. (Figure 6). The chemical shift as well as the observed $^2J(\text{F},\text{P})$ and $^1J(\text{F},\text{Pt})$ coupling constants are typical for a platinum bound fluoro ligand with phosphorus nuclei in a *trans* or *cis* arrangement.^[1d,e,5c,6h,j] In the ^{19}F NMR spectrum the signal gets broadened to a doublet with ^{195}Pt satellites, in part due to the coupling to the NH proton and HF. Additionally, a broad signal for remaining $(\text{HF})_4$ was found at $\delta = -181.7$ ppm. The ^1H NMR spectrum of $5\cdot(\text{HF})_4$ displays a doublet at $\delta = 9.18$ ppm with a coupling constant of $J(\text{H},\text{F}) = 5.8$ Hz, indicating hydrogen bonding from the NH group to the fluoro ligand. The signal collapses to a singlet in the $^1\text{H}\{^{19}\text{F}\}$ NMR spectrum. Complex $5\cdot(\text{HF})_4$ was treated with CsF for 5 min to remove excess of HF. Indeed, the formation of the fluoride complex $\text{cis}[\text{PtF}\{\kappa^2\text{-}(P,N)\text{-iPr}_2\text{P}(\text{C}_9\text{H}_7\text{N})\}\{\text{iPr}_2\text{P}(\text{C}_9\text{H}_8\text{N})\}]$ (**5**) was observed, but also its precursor complex $\text{cis}[\text{Pt}\{\kappa^2\text{-}(P,N)\text{-iPr}_2\text{P}(\text{C}_9\text{H}_7\text{N})\}\{\text{iPr}_2\text{P}(\text{C}_9\text{H}_8\text{N})\}]$ (**4**) in a ratio of 1:1 as evidenced by the $^{31}\text{P}\{^1\text{H}\}$ NMR spectrum. For complex **5** the $^{19}\text{F}\{^1\text{H}\}$ NMR spectrum displays a doublet of doublets with ^{195}Pt satellites at $\delta = -282.5$ ppm revealing coupling constants of $^2J(\text{F},\text{P}) = 127.5$ Hz, $^2J(\text{F},\text{P}) = 7.4$ Hz and $^1J(\text{F},\text{Pt}) = 180$ Hz (Figure 7). In the ^{19}F NMR spectrum the signal appears as a doublet of doublets due to additional coupling with the NH proton exhibiting a $^1J(\text{F},\text{H})$ coupling constant of 26.7 Hz. For the NH proton a doublet is found at $\delta = 10.64$ ppm ($^1J(\text{H},\text{F}) = 26.7$ Hz) in the ^1H NMR spectrum, which collapses to a singlet in the $^1\text{H}\{^{19}\text{F}\}$ NMR spectrum. Note that the values of the $^1J(\text{F},\text{Pt})$ and $^2J(\text{F},\text{P})$ coupling constants decreased after the removal of

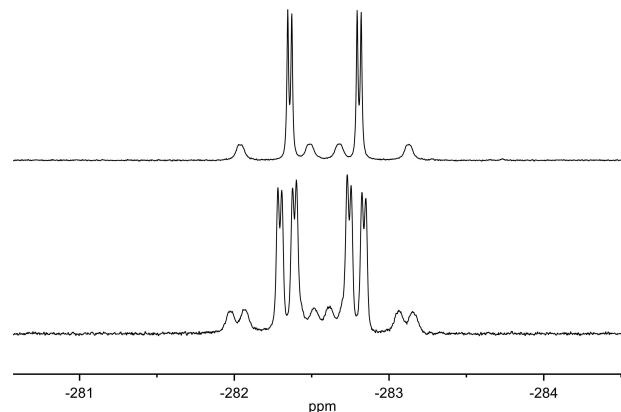


Figure 7. Part of the ^{19}F NMR spectrum (bottom) and the $^{19}\text{F}\{^1\text{H}\}$ NMR spectrum (top) of HF free $\text{cis}[\text{PtF}\{\kappa^2\text{-}(P,N)\text{-iPr}_2\text{P}(\text{C}_9\text{H}_7\text{N})\}\{\text{iPr}_2\text{P}(\text{C}_9\text{H}_8\text{N})\}]$ (**5**) revealing coupling constants of $^1J(\text{F},\text{H}) = 26.7$ Hz, $^2J(\text{F},\text{P}) = 126.5$ Hz, $^2J(\text{F},\text{P}) = 7.3$ Hz and $^1J(\text{F},\text{Pt}) = 180$ Hz.

HF, which might indicate that the bond has less s-orbital character. However, a larger $^1J(\text{H},\text{F})$ coupling constant was found, which indicates a stronger hydrogen bond from the NH proton to the fluorido ligand.

At room temperature a solution of fluorido complex $5 \cdot (\text{HF})_4$ was not stable and after 30 minutes the formation of the complex *cis*-[Pt(2-C₉H₈N){κ²-(P,N)-iPr₂P(C₉H₇N)}{iPr₂PF}] (**6**) bearing a fluorophosphine ligand was observed by a dyotropic rearrangement (Scheme 2). The ratio $5 \cdot (\text{HF})_4$: **6** was found to be 1 : 1.5 after approximately 90 minutes after addition of HF (as indicated by the signal intensity in the ¹⁹F NMR spectrum). Note, that this rearrangement reaction was not observed for the HF free complex **5** after 90 minutes. However, after 24 h complex **6** was detected in small amount with a ratio **5**:**6** of 4.5:1. A complete conversion to complex **6** was not achieved, since at the same time decomposition to yield a fluorophosphonium cation started, which was detected in the corresponding ¹⁹F NMR spectrum as a doublet of triplets at $\delta = -98.6$ ppm ($^1J(\text{F},\text{P}) = 1042.2$ Hz, $^3J(\text{F},\text{H}) = 6.8$ Hz) as well as in the ³¹P{¹H} NMR spectrum as a doublet at $\delta = 80.4$ ppm ($^1J(\text{P},\text{F}) = 1042.2$ Hz). Comparable $^1J(\text{F},\text{P})$ coupling constants are described in the literature for other fluorophosphonium salts.^[28]

The ¹⁹F NMR spectrum of **6** displays a doublet of doublet of triplets with ¹⁹⁵Pt satellites at $\delta = -143.7$ ppm revealing coupling to both phosphorus nuclei ($^1J(\text{F},\text{P}) = 854.8$ Hz, $^3J(\text{F},\text{P}) = 59.6$ Hz), the CH protons of the proximal isopropyl groups with a coupling constant of $^3J(\text{F},\text{H}) = 14.1$ Hz as well as coupling to the platinum centre with a coupling constant of $^2J(\text{F},\text{Pt}) = 401$ Hz. The signal collapses to a doublet of doublets with ¹⁹⁵Pt satellites in the ¹⁹F{¹H} NMR spectrum (Figure 8). The ³¹P{¹H} NMR spectrum features a strongly downfield shifted doublet of doublets with ¹⁹⁵Pt satellites for the fluorophosphine ligand at $\delta = 179.9$ ppm with coupling constants of $^1J(\text{P},\text{F}) = 854.8$ Hz, $^2J(\text{P},\text{P}) = 9.3$ Hz and $^1J(\text{P},\text{Pt}) = 3991$ Hz. Comparable data for fluorophosphine ligands have been described by Schmutzler et al. as well as Perutz, Braun et al. for platinum(II) complexes, Macgregor, Grushin et al. for rhodium(I) complexes and Milstein et al. for iridium(I) complexes.^[29] For the phosphorus atom of

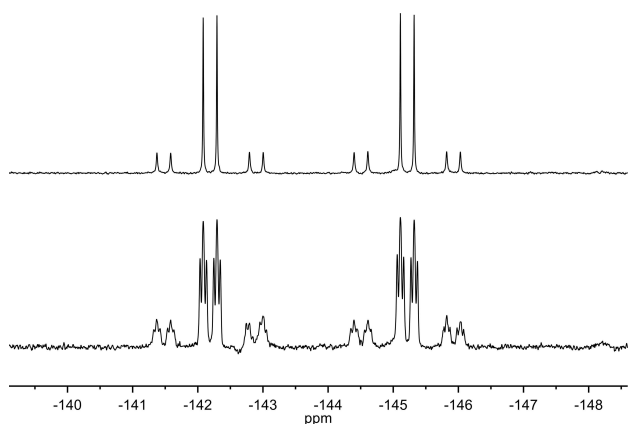


Figure 8. Part of the ¹⁹F NMR (bottom) and the ¹⁹F{¹H} NMR spectrum (top) of *cis*-[Pt(2-C₉H₈N){κ²-(P,N)-iPr₂P(C₉H₇N)}{iPr₂PF}] (**6**) revealing coupling constants of $^1J(\text{F},\text{P}) = 854.8$ Hz, $^3J(\text{F},\text{P}) = 59.6$ Hz, $^3J(\text{F},\text{H}) = 14.1$ Hz and $^2J(\text{F},\text{Pt}) = 401$ Hz.

the cyclometalated phosphine, a doublet of doublets with ¹⁹⁵Pt satellites is found at $\delta = 7.0$ ppm with coupling constants of $^3J(\text{P},\text{F}) = 59.6$ Hz, $^2J(\text{P},\text{P}) = 9.3$ Hz. The small $^1J(\text{P},\text{Pt})$ coupling constant of 1498 Hz gives an additional indication for a phosphorus atom *trans*-bound to an σ -aryl donor ligand.^[30]

Reactivity of *cis*-[PtF{κ²-(P,N)-iPr₂P(C₉H₇N)}{iPr₂P(C₉H₈N)}] (**5**·(HF)₄) towards CO.

Next, the reactivity of complex $5 \cdot (\text{HF})_4$ towards carbon monoxide was studied to estimate the binding properties of the fluoride ligand. Exposure of an in situ formed solution of complex $5 \cdot (\text{HF})_4$ to an atmosphere of CO resulted in the formation of the complex *trans*-[Pt(CO){κ²-(P,C)-iPr₂P(C₉H₇NCO)}{iPr₂P(C₉H₈N)}][F(HF)₄] (**7**) (Scheme 2). Apparently, an insertion of a CO molecule into the Pt–N bond occurred in addition to CO coordination at the Pt centre, resulting in a five membered carbamoyl metallacycle. The presence of an excess of HF, which forms a poly(hydrogen fluoride) anion, is necessary for the generation and stabilisation of the fluoride anion and, therefore, complex **7** in solution. Accordingly, addition of CsF to complex **7** resulted in a second cyclometallation yielding *trans*-[Pt{κ²-(P,C)-iPr₂P(C₉H₇NCO)}]₂ (**8**) as the only product (Scheme 2). Note that an independent reaction of complexes **3** and **4** with CO did not show any conversion.

The ³¹P{¹H} NMR spectra of **7** and **8** feature downfield shifted signals with ¹⁹⁵Pt satellites at $\delta = 55.7$, 31.8 ppm and 47.8 ppm, respectively. In the ¹H NMR spectrum a broad signal at $\delta = 10.82$ ppm is observed, which can be assigned to F(HF)₄[−] anion.^[27b] For the NH proton a signal at $\delta = 10.61$ ppm is observed featuring a downfield shift through hydrogen bonding with the poly(hydrogen fluoride) anion.^[13b] The IR spectrum of complex **7** features a very intense absorption band at $\tilde{\nu} = 2108$ cm^{−1}, which can be attributed to the CO stretch of the CO ligand. Another band is observed at 1654 cm^{−1} resulting from the CO stretch of the carbamoyl group. Comparable stretching frequencies have been reported for other cationic Pt(II) carbonyl/carbamoyl complexes.^[31] Additionally, a broad absorption band could be identified at $\tilde{\nu} = 1797$ cm^{−1}, which can be assigned to the stretching vibrations of the poly(hydrogen fluoride) anion.^[32] The IR spectrum of **8** displayed an absorption band at $\tilde{\nu} = 1664$ cm^{−1}, which is assigned to the CO stretch of the carbamoyl group. The molecular structure of *trans*-[Pt{κ²-(P,C)-iPr₂P(C₉H₇NCO)}]₂ (**8**) was also determined by X-ray crystal structure determination (Figure 9). It features a slightly distorted square-planar coordination of the cyclometalated phosphine ligand, as represented by the C1–Pt1–P1 angle of 85.51(9)°. The P1–Pt1 length of 2.2833(8) Å is comparable with the P–Pt distance found for the *trans* complex **2**. The Pt–C1 bond length is found to be 2.056(3) Å. A C1–O1 bond length of 1.219(4) Å and a N1–C1 1.442(4) Å is observed for the carbamoyl group. Similar bond lengths were reported for other platinum carbamoyl complexes.^[33]

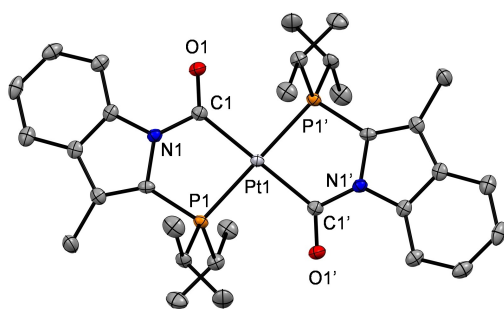
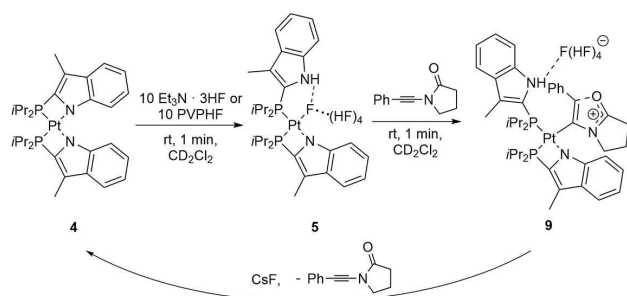


Figure 9. Structure of *trans*-[Pt{ κ^2 -(*P,C*)-*iPr*₂P(C₉H₇NCO)}₂] (**8**). Thermal ellipsoids are drawn at 50% probability level. Hydrogen atoms were omitted for clarity. Selected distances (Å) and angles (°): Pt1–P1 2.2833(8); Pt1–C1 2.056(3); P1–C2 1.808(3); N1–C2 1.416(4); N1–C1 1.442(4); C1–O1 1.219(4); C1–Pt1–P1 85.51(9); C1–Pt1–P1' 94.49(9).

Reactivity of *cis*-[PtF{ κ^2 -(*P,N*)-*iPr*₂P(C₉H₇N)}]{*iPr*₂P(C₉H₈N)}] (**5**·(HF)₄) towards an Ynamide

Additionally, the reactivity of the platinum fluoro complex **5**·(HF)₄ towards alkynes and amino substituted alkynes (ynamides) was studied. In the past several examples for the transition metal catalysed hydrofluorination of alkynes and ynamides were reported. However, these reactions are limited solely to Au(I) complexes^[2c,26b,34] and to some extent on Ag(I)/Cu(I) complexes as catalytic precursors.^[35]

Initially, an in situ generated reaction solution of complex **5**·(HF)₄ was treated with diphenylacetylene or phenylacetylene, but no reactions with the substrates were observed and the rearrangement reaction to give complex **6** took place. However, a reaction of in situ formed complex **5**·(HF)₄ with one equivalent of 1-(2-phenylethynyl)-2-pyrrolidinone led to the selective formation of a Pt(II) complex, for which the spectroscopic data are consistent with the compound *cis*-[Pt{C=C(Ph)OCN(C₃H₆)}{ κ^2 -(*P,N*)-*iPr*₂P(C₉H₇N)}]{*iPr*₂P(C₉H₈N))}] [F(HF)₄] (**9**), which results from a cyclisation of the ynamide at the platinum centre. (Scheme 3). For its generation a metallaketeneiminium moiety can be discussed as intermediate.^[36] As described for complex **7**, complex **9** requires an excess of HF to stabilise a poly(hydrogen fluoride) anion in the coordination sphere. Hence, addition of CsF did not lead to the fluorination of the carbon α to the nitrogen, but gave cyclometallation to yield complex **4**,



Scheme 3. Reactivity of the fluoro complex **5**·(HF)₄ towards 1-(2-phenylethynyl)-2-pyrrolidinone.

and the release of 1-(2-phenylethynyl)-2-pyrrolidinone was observed instead. Note, that the HF free complex **5** and also compound **3** showed no reactivity towards the ynamide.

Complex **9** was characterised by its NMR and IR data together with DFT calculations. Experimentally, the ³¹P{¹H} NMR spectrum of complex **9** features two doublets with ¹⁹⁵Pt satellites at δ = 11.6 ppm and –3.1 ppm with a ²J(*P,P*) coupling constant of 15.8 Hz and ¹J(*P,Pt*) coupling constants of 3112 Hz and 1892 Hz, respectively. The low value of 1892 Hz found for the ¹J(*P,Pt*) coupling constant indicates the presence of a σ -carbon donor ligand in the *trans* position.^[30b] In the ¹⁹F NMR spectrum, a signal at δ = –174.3 ppm was detected, which indicates the presence of a poly(hydrogen fluoride) entity.^[27,37] The corresponding signal in the ¹H NMR spectrum can be found at δ = 10.77 ppm. Most likely this suggests the presence of an F(HF)₄[–] anion.^[27b] For the nitrogen bound proton a resonance signal is found at δ = 10.22 ppm. The signal of the NH proton appears strongly downfield shifted suggesting hydrogen bonding with the poly(hydrogen fluoride) anion.^[13b] Furthermore, the ¹H NMR spectrum displays six signals which could be assigned via a ¹H,¹H COSY NMR experiment to the three CH₂ moieties of the pyrrolidinone backbone. For the two carbon atoms of the Pt–C=C moiety two doublets of doublets were detected in the ¹³C{¹H} NMR at 160.3 (C β to Pt) and 123.9 ppm (C α to Pt). The ¹H/¹⁵N HMBC spectrum of **9** reveals cross peaks at 10.22/–245 (d/s, ¹J(NH) = 97.8 Hz, *N-H*) and at 3.24/–163 (s/s), 3.13/–163 (s/s) ppm. The latter signal at –163 ppm can be assigned to the nitrogen of the pyrrolidinone backbone. Note that the ¹⁵N chemical shift of free 1-(2-phenylethynyl)-2-pyrrolidinone was detected at –269 ppm (Figure S42). A signal for the platinum bound nitrogen atom could not be detected.

The IR spectrum of complex **9** displays a broad absorption band at 3263 cm^{–1} which can be attributed to the N–H stretch (Figure 10). As it was already described for complex **7** a broad absorption band was detected at $\tilde{\nu}$ = 1801 cm^{–1} for the stretching vibrations of the poly(hydrogen fluoride) anion.^[32] Further data were obtained from liquid injection field desorption/ionisation mass spectrometry (LIFDI-MS). The mass spec-

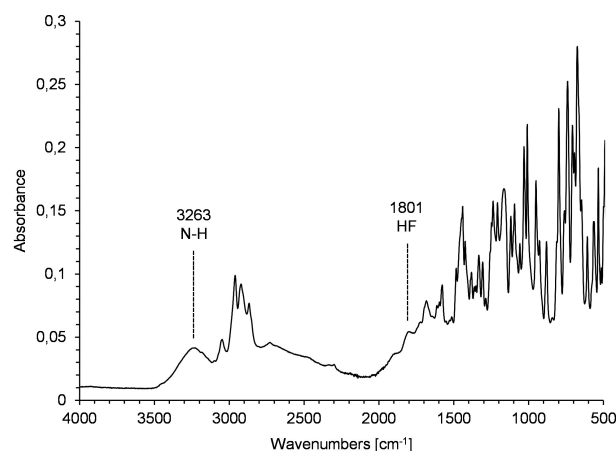
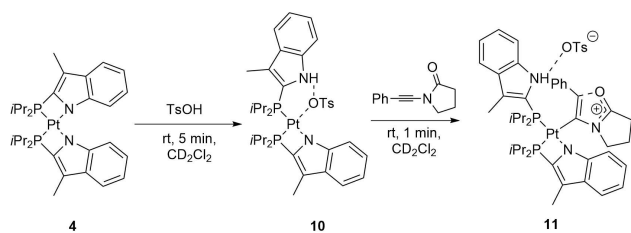


Figure 10. IR spectrum of *cis*-[Pt{C=C(Ph)OCN(C₃H₆)}{ κ^2 -(*P,N*)-*iPr*₂P(C₉H₇N)}]{*iPr*₂P(C₉H₈N))}] [F(HF)₄] (**9**).



Scheme 4. Formation of the tosylate complex **10** and its reactivity towards 1-(2-phenylethynyl)-2-pyrrolidinone.

trum revealed a peak at $m/z = 873.507$ which can be assigned to the complex cation $[M]^+$ (calcd. 873.339).

To gain further insight into the activation of the ynamide, the tosylate ($\text{OTs}^- = \text{H}_3\text{CC}_6\text{H}_4\text{SO}_3^-$) complex $\text{cis-}[\text{Pt}\{\kappa^2\text{-}(P,N)\text{-}i\text{Pr}_2\text{P}\text{-}(\text{C}_9\text{H}_7\text{M})\}\{i\text{Pr}_2\text{P}(\text{C}_9\text{H}_8\text{N})\}][\text{OTs}]$ (**10**) (Scheme 4) was treated with 1-(2-phenylethynyl)-2-pyrrolidinone to give $\text{cis-}[\text{Pt}\{\text{C}=\text{C}(\text{Ph})\text{OCN}(\text{C}_3\text{H}_6)\}\{\kappa^2\text{-}(P,N)\text{-}i\text{Pr}_2\text{P}(\text{C}_9\text{H}_7\text{M})\}\{i\text{Pr}_2\text{P}(\text{C}_9\text{H}_8\text{N})\}][\text{OTs}]$ (**11**). Compound **10** was prepared from **4** on treatment with HOTs. Complex **11** revealed comparable data to complex **9** from its $^31\text{P}\{^1\text{H}\}$ NMR, $^{13}\text{C}\{^1\text{H}\}$ NMR and $^1\text{H}/^{15}\text{N}$ HMBC spectra. In the IR spectrum of **11**

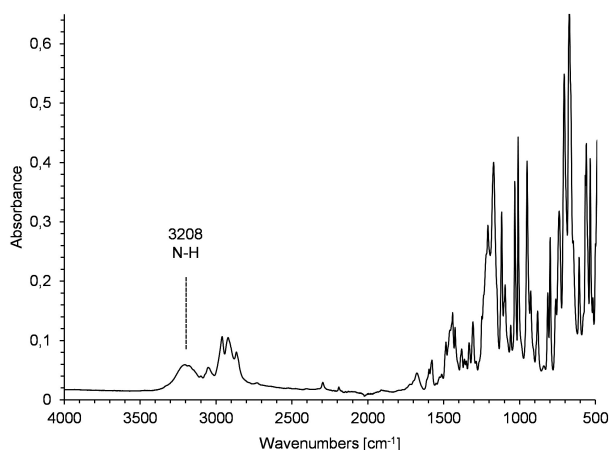


Figure 11. IR spectrum of $\text{cis-}[\text{Pt}\{\text{C}=\text{C}(\text{Ph})\text{OCN}(\text{C}_3\text{H}_6)\}\{\kappa^2\text{-}(P,N)\text{-}i\text{Pr}_2\text{P}(\text{C}_9\text{H}_7\text{M})\}\{i\text{Pr}_2\text{P}(\text{C}_9\text{H}_8\text{N})\}][\text{OTs}]$ (**11**).

an absorption band at $\tilde{\nu} = 3208 \text{ cm}^{-1}$ was found for the N–H stretch (Figure 11).

Note that the interpretation of the experimental NMR and IR data of **9** and **11** is not consistent with alternative structures such as alkyne or keteniminium complexes or any structure resulting from C–F or C–OTs bond formation, as will be revealed by the discussion of the computational results below. An overview of selected experimental and calculated NMR and IR data is provided in Table 2. A complete overview of all the calculated data for a variety of conceivable complex isomers of **9** and **11** is listed in Tables S2–S5. In short, the absence of a $^1J(\text{F},\text{C})$ coupling constant at any metal-bound organyl moiety clearly excludes the formation of a C–F bond in **9**. The presence of a metal-bound alkyne complex can be excluded by the ^{13}C NMR data. The absence of a stretching mode for $\text{C}=\text{C}=\text{N}$ in the experimental (solid state and liquid phase; *c.f.* Figure S37) IR spectra as well as the ^{15}N NMR data disfavour the generation of a keteniminium complex. The same considerations hold true for the NMR data and the IR spectra of complex **11** (Figure S39).

These latter assumptions are primarily based on DFT computations of the IR spectroscopic data, NMR chemical shifts, as well as thermochemical data for a variety of possible products of the reactions of **5** or **10** with the ynamide (comprehensive details are provided in the Supporting Information). An accurate quantum chemical treatment of the poly (hydrogen fluoride) anion is particularly demanding. Since the experimental NMR and IR spectroscopic data sets appear essentially equal for both the $\text{F}(\text{HF})_4^-$ (**9**) and tosylate (**11**) ynamide complexes, the computations mainly focused on analyses of the latter compound.

Initially, IR data were analysed for the products of a metal-free reaction of *p*-toluenesulfonic acid with 1-(2-phenylethynyl)-2-pyrrolidinone, which has also been conducted experimentally. An overlay of the computed IR spectra of the reactant, the intermediately formed unstable tosylate-keteniminium contact ion pair, and the final 1,2-addition product is shown in Figure 12. The overall reaction is calculated to be strongly exergonic by -81 kJ/mol , and hence proceeds irreversibly at ambient conditions in solution (detailed thermochemical and kinetic data for the reaction in dichloromethane are provided in Scheme S1).

Table 2. Selected experimental NMR and IR data for the complexes **9** and **11**, and calculated data for alternative metallaketenimines and alkyne complexes; Figure 13 shows the corresponding calculated structures.

structure	compound	$\delta(^{13}\text{C} / ^{15}\text{N})^{[a,b]}$		C3	N1	N2	N3	normal mode ^[c]		
		C1	C2					$\tilde{\nu}(\text{C}=\text{C})$	$\tilde{\nu}(\text{CCN } as)$	$\tilde{\nu}(\text{CO})$
experimental	11	160.3	123.9	170.3	–163	–245	–	–	–	–
		159.9	123.6	170.9	–163	–243	–	–	–	–
COSMO(DCM)	9-1	82	82	190	–274	–246	–225	2046	–	1668
	9-2	93	164	183	–255	–258	–232	–	1991	1770
	9-3	175	142	178	–168	–258	–230	–	–	–
	11-1	86	116	189	–267	–242	–234	2015	–	1722
	11-2	86	141	193	–259	–247	–243	–	2021	1745
	11-3	173	138	181	–168	–254	–236	–	–	–

[a] Molecular and atomic labels are depicted in Figure 13; [b] Fully relativistic 4c-mDKS/PBE0/Dyall-VTZ/IGLO-III/IGLO-II calculations at MARIJ-BP86-D3(BJ)/def2-TZVP/COSMO(DCM) optimized structures. References: TMS (^{13}C), CH_3NO_2 (^{15}N); [c] Harmonic vibrational frequency analyses at MARIJ-BP86-D3(BJ)/def2-TZVP/COSMO(DCM) optimized structures.

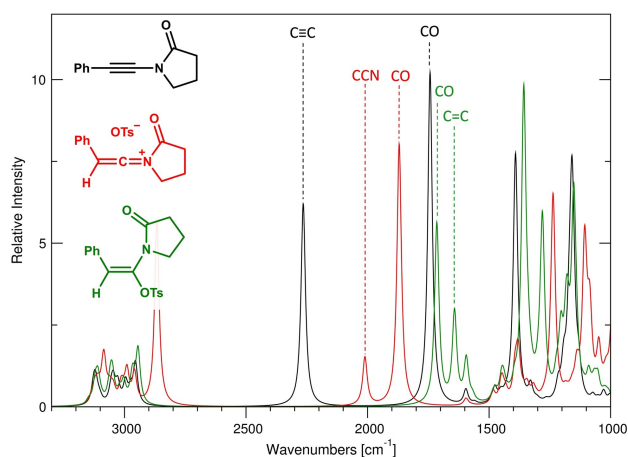


Figure 12. Calculated IR spectra of 1-(2-phenylethynyl)-2-pyrrolidinone and its reaction products with *p*-toluenesulfonic acid (MARIJ-BP86-D3(BJ)/def2-TZVP level).

The ynamide itself shows a strong band for the ethynyl triple bond at $\tilde{\nu} = 2265 \text{ cm}^{-1}$ (experimental: $\tilde{\nu} = 2240 \text{ cm}^{-1}$). Upon formation of the keteniminium tosylate contact ion pair, a weaker but nevertheless distinct band at $\tilde{\nu} = 2011 \text{ cm}^{-1}$ for the asymmetric CCN stretching vibration is observed, accompanied by a considerable blue shift of the CO band of about 130 cm^{-1} . Importantly, the presence of the tosylate anion in close vicinity to the CCN^+ moiety does not affect the CCN band significantly. Comparison with the corresponding IR band of the free keteniminium cation shows that the impact of the anion on the CCN stretching vibration within the contact ion pair unit is merely about 30 cm^{-1} (Table S1), with little effect on its intensity. It is only upon covalent bond formation between one of the tosylate oxygen atoms and the α -N carbon atom, and hence a concomitant C=C bond formation, that the CCN band vanishes from the spectrum. At the same time the CO band is significantly shifted back again to lower frequencies by about 150 cm^{-1} . These results evidently suggest that a similarly strong interaction, like a 1,2-addition type reaction, is likely the cause for the absence of a CCN band in the experimental spectra of the platinum ynamide complexes. Note, however, that unlike the product from the metal-free conversion of the ynamide with TsOH, complexes **9** and **11** do not exhibit an explicit CO band in the range of $1600\text{--}1900 \text{ cm}^{-1}$, as revealed by a closer analysis of their IR spectroscopic data (by comparison with the IR spectrum of **4**, Figure S44).

Analyses of the structural and conformational space of **11** naturally shows a more complicated stereochemical situation, which is mainly caused by the high flexibility of the ynamide and the anion in terms of their (mutual) structural arrangements within the metal complex. In general, the computed isomers can be divided into two categories: structures which feature a metallaketeniminium or metallacyclopropene motif, that is, a coordinated alkyne (**11-1–11-2** in Figure 13), and structures exhibiting a vinyl binding motif from 1,2 addition at the ynamide. This involves structures resulting from insertion of the ynamide into the Pt–N bond of **10** (affording **11-10**, Table S3),

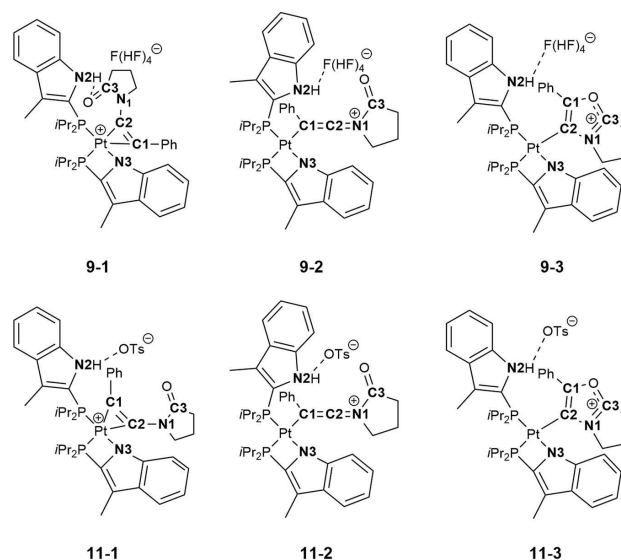


Figure 13. Selected calculated schematic structure representations with atomic labels used to indicate corresponding ^{13}C / ^{15}N NMR atomic shifts (Table 2) of conceivable reaction products of the reactions of 5-(HF)₄ or **10** with 1-(2-phenylethynyl)-2-pyrrolidinone (MARIJ-BP86-D3(BJ)/def2-TZVP results).

addition of the anion at the α -N carbon atom of the keteniminium moiety in **11-2** (structures **11-6** and **11-7** in Table S3), cyclisation of **11-2** involving the keteniminium and the indolyl ligand (**11-8** and **11-9** in Table S3), and intra-ligand cyclisation of the keteniminium moiety in **11-2**, leading to **11-3** (Figure 13). From a purely thermochemical point of view, the latter structure is more stable when compared to the corresponding metallaketeniminium or metallacyclopropene isomers. Note, that this does not imply that they are all necessarily kinetically accessible under the experimental conditions. However, metallaketeniminium or metallacyclopropene structures are likely formed intermediately upon initial ynamide coordination, serving as starting point for subsequent transformations.

Closer inspection of the computed IR data of all isomers provides further evidence for the structural characteristics of **11**. Firstly, in accordance with the results from the reaction of 1-(2-phenylethynyl)-2-pyrrolidinone with TsOH, only the spectra of those structures accessed by a 1,2 addition at the ynamide are void of a dominant CCN band. Secondly, due to the metal-assisted intramolecular ring closure by means of the pyrrolidinone CO group, isomer **11-3** is the only structure which does not exhibit a distinct CO band, in agreement with the experimental findings (*c.f.* Figure S44). Figure 14 provides a comparison of calculated data for two representative configurations (**11-2** and **11-3**, *c.f.* Table S3).

Additional evidence which puts **11-3** in favour over alternative structural motifs is provided by the calculated NMR chemical shifts. As can be seen from Table 2, the ^{13}C NMR shifts are not consistent with alkyne (**11-1**) or metallaketeniminium (**11-2**) complexes (additional data are provided in Tables S2 and S4). More importantly, the experimental ^{15}N NMR data reveal a

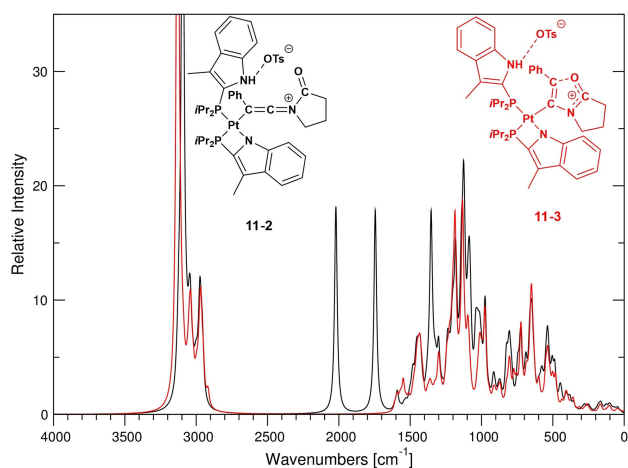


Figure 14. Calculated IR spectra of exemplary platinum ynamide complex conformers from reaction of **10** with 1-(2-phenylethynyl)-2-pyrrolidinone (MARIJ-BP86-D3(BJ)/def2-TZVP level).

significant high-frequency-shift for the nitrogen atom N1 of the ynamide upon coordination. This particularly characteristic feature is only seen for the keteniminium moiety after ring closure in isomer **11-3**. The same considerations hold for the derivatives with polyfluorido moieties instead of a tosylate (**9-1-9-3**, Table 2).

Inter- and intramolecular (electro-)cyclisation reactions using keteniminium salts as intermediates are seeing widespread use in organic chemistry, and corresponding synthesis procedures involving complexes of late transition metals are common.^[36d,e,h-j] These also involve intramolecular trapping of (metalated) keteniminium ions, which further supports the identification of **11-3** as platinum-bound cyclic keteniminium species.

Additionally, the plausibility of the intra-ligand cyclisation mechanism was corroborated by modeling of the corresponding free energy profile (Scheme S2). The overall reaction proceeds strongly exergonically, by -71 kJ mol^{-1} , and the computed barrier for cyclisation of 66 kJ mol^{-1} is fully consistent with a process at room temperature. In line with the observed reversibility of complex formation upon treatment of **9** with CsF (Scheme 3), calculations show that the free ligand of **9** easily rearranges to the significantly more stable alkyne structure, with a barrier for ring opening of only 34 kJ mol^{-1} (Scheme S2).

Conclusion

In conclusion, we described the formation of various platinum (II) complexes bearing κ^1 -(P)- and κ^2 -(P,N)- bound diisopropyl-2-(3-methyl)indolyl phosphine ligands and their reactivity towards fluorides as well as hydrogen fluoride. The metal bound fluorides can induce cyclometallation, migrate to phosphorous and engage in hydrogen bonding to NH units or generate polyfluorido moieties. The reaction of cis -[PtCl₂{iPr₂P(C₉H₈N)}₂] (**1**) and cis -[PtCl{ κ^2 -(P,N)-iPr₂P(C₉H₇N)}]{iPr₂P(C₉H₈N)} (**3**) with

tetramethylammonium fluoride (TMAF) yielding the twofold cyclometallated complex cis -[Pt{ κ^2 -(P,N)-iPr₂P(C₉H₇N)}₂] (**4**) demonstrated the ability of free fluorides to react as a nucleophile and a base, which is consistent with the literature.^[24a,b,d,38] Reaction of complex **4** with hydrogen fluoride sources (Et₃N·3HF or PVPFH) resulted in the formation of the unique platinum fluoro complex **5**·(HF)₄, which exhibits outer-sphere hydrogen bonding between the fluoro ligand and an indolyl unit as well as several HF molecules. In contrast to its chlorido analogue **3**, the fluoro complex **5**·(HF)₄ reacted with CO and the ynamide 1-(2-phenylethynyl)-2-pyrrolidinone leading to the carbamoyl complex $trans$ -[Pt(CO){ κ^2 -(P,C)-iPr₂P(C₉H₇NCO)}]{iPr₂P(C₉H₈N)}[F(HF)₄] (**7**) and the complex cis -[Pt{C=C(Ph)OCN(C₃H₆)}]{ κ^2 -(P,N)-iPr₂P(C₉H₇N)}]{iPr₂P(C₉H₈N)}[F(HF)₄] (**9**). Pendant hydrogen fluoride in **5**·(HF)₄ was found to be important to enable both reactions through stabilisation of the released fluoride as a F(HF)₄⁻ anion in the coordination sphere and preventing further cyclometallation. Thus, hydrogen bonding in the outer ligand sphere controls the reactivity of fluoro complexes and this might provide new pathways for transition metal mediated fluorination reactions.

Experimental Section

Full details of experimental procedures, complex synthesis and characterisation, NMR data, IR data and crystallographic data as well as computational details can be found in the Supporting Information.

Deposition Number(s) 2049732 (for **1-2** CH₂Cl₂), 2049734 (2·C₇H₈), 2062626 (for **2-2** C₄H₈O), 2049731 (for **3**·C₇H₈), 2049733 (for **4**), 2049730 (for **8**) contain(s) the supplementary crystallographic data for this paper. These data are provided free of charge by the joint Cambridge Crystallographic Data Centre and Fachinformationszentrum Karlsruhe Access Structures service.

Acknowledgements

We gratefully acknowledge financial support from the CRC 1349 funded by the Deutsche Forschungsgemeinschaft (DFG, German Research Foundation; Gefördert durch die Deutsche Forschungsgemeinschaft – Projektnummer 387284271 – SFB 1349). We would like to thank Dr. A. Dallmann and R. Jaeger for measurements of the ¹H,¹⁵N HMBC NMR spectra. We also wish to thank N. Pfister for the low-temperature NMR measurements and acknowledge M. Wozniak as well as S. Rachor for scientific discussions. Open Access funding enabled and organized by Projekt DEAL.

Conflict of Interest

The authors declare no conflict of interest.

Keywords: fluoro complexes · hydrogen bonding · phosphine · platinum · polyfluorides

- [1] a) N. M. Doherty, N. W. Hoffmann, *Chem. Rev.* **1991**, *91*, 553–573; b) E. F. Murphy, R. Murugavel, H. W. Roesky, *Chem. Rev.* **1997**, *97*, 3425–3468; c) V. V. Grushin, *Chem. Eur. J.* **2002**, *8*, 1006–1014; d) P. Nilsson, F. Plamper, O. F. Wendt, *Organometallics* **2003**, *22*, 5235–5242; e) A. Yahav, I. Goldberg, A. Vignalok, *Inorg. Chem.* **2005**, *44*, 1547–1553; f) T. Braun, A. Steffen, V. Schorlemer, B. Neumann, H.-G. Stammler, *Dalton Trans.* **2005**, 3331–3336; g) D. S. Laitar, P. Müller, T. G. Gray, J. P. Sadighi, *Organometallics* **2005**, *24*, 4503–4505; h) D. A. Watson, M. Su, G. Teverovskiy, Y. Zhang, J. García-Fortanet, T. Kinzel, S. L. Buchwald, *Science* **2009**, *325*, 1661; i) A. Vignalok, *Organometallics* **2011**, *30*, 4802–4810; j) E. Clot, O. Eisenstein, N. Jasim, S. A. Macgregor, J. E. McGrady, R. N. Perutz, *Acc. Chem. Res.* **2011**, *44*, 333–348; k) D. A. Smith, T. Beweries, C. Blasius, N. Jasim, R. Nazir, S. Nazir, C. C. Robertson, A. C. Whitwood, C. A. Hunter, L. Brammer, R. N. Perutz, *J. Am. Chem. Soc.* **2015**, *137*, 11820–11831; l) M. G. Campbell, T. Ritter, *Chem. Rev.* **2015**, *115*, 612–633; m) H. Baumgarth, G. Meier, T. Braun, B. Braun-Cula, *Eur. J. Inorg. Chem.* **2016**, *2016*, 4565–4572; n) T. Ahrens, J. Kohlmann, M. Ahrens, T. Braun, *Chem. Rev.* **2015**, *115*, 931–972; o) J. Kohlmann, T. Braun, R. Laubenstein, R. Herrmann, *Chem. Eur. J.* **2017**, *23*, 12218–12232.
- [2] a) A. C. Albéniz, J. A. Casares, in *Adv. Organomet. Chem.*, Vol. 62 (Ed.: P. J. Pérez), Academic Press, **2014**, pp. 1–110; b) K. M. Engle, T.-S. Mei, X. Wang, J.-Q. Yu, *Angew. Chem. Int. Ed.* **2011**, *50*, 1478–1491; *Angew. Chem.* **2011**, *123*, 1514–1528; c) J. A. Akana, K. X. Bhattacharyya, P. Müller, J. P. Sadighi, *J. Am. Chem. Soc.* **2007**, *129*, 7736–7737.
- [3] a) M. Talavera, C. N. von Hahmann, R. Müller, M. Ahrens, M. Kaupp, T. Braun, *Angew. Chem. Int. Ed.* **2019**, *58*, 10688–10692; *Angew. Chem.* **2019**, *131*, 10798–10802; b) M. Talavera, R. Müller, T. Ahrens, C. N. von Hahmann, B. Braun-Cula, M. Kaupp, T. Braun, *Faraday Discuss.* **2019**, *220*, 328–349; c) M. Talavera, T. Braun, *Synlett* **2020**, *31*, 1760–1774.
- [4] a) J. M. Mayer, *Comments Inorg. Chem.* **1988**, *8*, 125–135; b) K. G. Caulton, *New J. Chem.* **1994**, *18*, 25–41; c) P. L. Holland, R. A. Andersen, R. G. Bergman, *Comments Inorg. Chem.* **1999**, *21*, 115–129.
- [5] a) R. D. W. Kemmitt, R. D. Peacock, J. Stocks, *J. Chem. Soc. A* **1971**, 846–849; b) K. R. Dixon, J. J. McFarland, *J. Chem. Soc. Chem. Commun.* **1972**, 1274–1275; c) M. A. Cairns, K. R. Dixon, J. J. McFarland, *J. Chem. Soc. Dalton Trans.* **1975**, 1159–1164; d) J. Howard, P. Woodward, *J. Chem. Soc. Dalton Trans.* **1973**, 1840–1843.
- [6] a) N. A. Jasim, R. N. Perutz, *J. Am. Chem. Soc.* **2000**, *122*, 8685–8693; b) T. Wang, B. J. Alfonso, J. A. Love, *Org. Lett.* **2007**, *9*, 5629–5631; c) T. Wang, J. A. Love, *Organometallics* **2008**, *27*, 3290–3296; d) A. Yahav-Levi, I. Goldberg, A. Vignalok, *J. Fluorine Chem.* **2010**, *131*, 1100–1102; e) A. D. Sun, J. A. Love, *J. Fluorine Chem.* **2010**, *131*, 1237–1240; f) T. Wang, L. Keyes, B. O. Patrick, J. A. Love, *Organometallics* **2012**, *31*, 1397–1407; g) R. Friedemann, K. Seppelt, *Eur. J. Inorg. Chem.* **2013**, *2013*, 1197–1206; h) J. Berger, T. Braun, R. Herrmann, B. Braun, *Dalton Trans.* **2015**, *44*, 19553–19565; i) A. Abo-Amer, P. D. Boyle, R. J. Puddephatt, *Inorg. Chem. Commun.* **2015**, *61*, 193–196; j) J. Berger, T. Braun, T. Ahrens, P. Kläring, R. Laubenstein, B. Braun-Cula, *Chem. Eur. J.* **2017**, *23*, 8886–8900; k) N. Arnold, R. Bertermann, F. M. Bickelhaupt, H. Braunschweig, M. Drisch, M. Finze, F. Hupp, J. Poater, J. A. P. Sprengrer, *Chem. Eur. J.* **2017**, *23*, 5948–5952; l) J. Hu, M. Nikraves, H. R. Shahsavari, R. Babadi Aghakhanpour, A. L. Rheingold, M. Alshami, Y. Sakamaki, H. Beyzavi, *Inorg. Chem.* **2020**, *59*, 16319–16327; m) E. Sarkissian, M. Golbon Haghighi, *Inorg. Chem.* **2021**, *60*, 1016–1020.
- [7] a) J.-W. Lee, M. T. Oliveira, H. B. Jang, S. Lee, D. Y. Chi, D. W. Kim, C. E. Song, *Chem. Soc. Rev.* **2016**, *45*, 4638–4650; b) S. Liang, G. B. Hammond, B. Xu, *Chem. Eur. J.* **2017**, *23*, 17850–17861; c) D. W. Kim, H.-J. Jeong, S. T. Lim, M.-H. Sohn, *Angew. Chem. Int. Ed.* **2008**, *47*, 8404–8406; *Angew. Chem.* **2008**, *120*, 8532–8534; d) C. Hollingworth, V. Gouverneur, *Chem. Commun.* **2012**, *48*, 2929–2942.
- [8] a) T. G. Richmond, *Coord. Chem. Rev.* **1990**, *105*, 221–250; b) C. E. Osterberg, M. A. King, A. M. Arif, T. G. Richmond, *Angew. Chem. Int. Ed. Engl.* **1990**, *29*, 888–890; *Angew. Chem.* **1990**, *102*, 960–961.
- [9] a) M. K. Whittlesey, R. N. Perutz, B. Greener, M. H. Moore, *Chem. Commun.* **1997**, 187–188; b) T. Braun, S. P. Foxon, R. N. Perutz, P. H. Walton, *Angew. Chem. Int. Ed.* **1999**, *38*, 3326–3329; *Angew. Chem.* **1999**, *111*, 3543–3545; c) S. J. Archibald, T. Braun, J. A. Gaunt, J. E. Hobson, R. N. Perutz, *J. Chem. Soc. Dalton Trans.* **2000**, 2013–2018; d) N. A. Jasim, R. N. Perutz, S. P. Foxon, P. H. Walton, *J. Chem. Soc. Dalton Trans.* **2001**, 1676–1685; e) F. Nahra, M. Brill, A. Gómez-Herrera, C. S. J. Cazin, S. P. Nolan, *Coord. Chem. Rev.* **2016**, *307*, 65–80; f) M. Joks, J. Haak, A. Spannenberg, T. Beweries, *Eur. J. Inorg. Chem.* **2017**, *2017*, 3815–3822.
- [10] a) B. P. Patel, R. H. Crabtree, *J. Am. Chem. Soc.* **1996**, *118*, 13105–13106; b) D.-H. Lee, H. J. Kwon, B. P. Patel, L. M. Liable-Sands, A. L. Rheingold, R. H. Crabtree, *Organometallics* **1999**, *18*, 1615–1621; c) J. H. Shin, G. Parkin, *Organometallics* **1998**, *17*, 5689–5696; d) S. Libri, N. A. Jasim, R. N. Perutz, L. Brammer, *J. Am. Chem. Soc.* **2008**, *130*, 7842–7844; e) A. Maity, R. J. Stanek, B. L. Anderson, M. Zeller, A. D. Hunter, C. E. Moore, A. L. Rheingold, T. G. Gray, *Organometallics* **2015**, *34*, 109–120; f) J. M. Stauber, G. E. Alliger, D. G. Nocera, C. C. Cummins, *Inorg. Chem.* **2017**, *56*, 7615–7619; g) C. M. Moore, N. K. Szymczak, *Chem. Commun.* **2015**, *51*, 5490–5492.
- [11] J. R. Wilson, M. Zeller, N. K. Szymczak, *Chem. Commun.* **2021**, *57*, 753–756.
- [12] a) J. Wessel, J. C. Lee Jr., E. Peris, G. P. A. Yap, J. B. Fortin, J. S. Ricci, G. Sini, A. Albinati, T. F. Koetzle, O. Eisenstein, A. L. Rheingold, R. H. Crabtree, *Angew. Chem. Int. Ed. Engl.* **1995**, *34*, 2507–2509; *Angew. Chem.* **1995**, *107*, 2711–2713; b) P. Desmurs, K. Kavallieratos, W. Yao, R. H. Crabtree, *New J. Chem.* **1999**, *23*, 1111–1115.
- [13] a) J. O. Yu, E. Lam, J. L. Sereda, N. C. Rampersad, A. J. Lough, C. S. Browning, D. H. Farrar, *Organometallics* **2005**, *24*, 37–47; b) J. O. Yu, C. S. Browning, D. H. Farrar, *Chem. Commun.* **2008**, 1020–1022.
- [14] a) E. Lam, D. H. Farrar, C. Scott Browning, A. J. Lough, *Dalton Trans.* **2004**, 3383–3388; b) I. O. Koshevoy, J. R. Shkairova, A. S. Melnikov, M. Haukka, S. P. Tunik, T. A. Pakkanen, *Dalton Trans.* **2011**, *40*, 7927–7933; c) Y.-Y. Kuo, M. F. Haddow, A. Pérez-Redondo, G. R. Owen, *Dalton Trans.* **2010**, *39*, 6239–6248; d) Y.-Y. Kuo, M. F. Haddow, A. L. Jamieson, G. R. Owen, *Transition Met. Chem.* **2013**, *38*, 641–648; e) Y.-Y. Kuo, R. C. Da Costa, H. A. Sparkes, M. F. Haddow, G. R. Owen, *Eur. J. Inorg. Chem.* **2020**, *2020*, 4195–4202.
- [15] P. G. Leviston, M. G. H. Wallbridge, *J. Organomet. Chem.* **1976**, *110*, 271–279.
- [16] a) S. O. Grim, R. L. Keiter, W. McFarlane, *Inorg. Chem.* **1967**, *6*, 1133–1137; b) A. Pidcock, R. E. Richards, L. M. Venanzi, *J. Chem. Soc. A* **1966**, 1707–1710; c) A. Pidcock, in *Catalytic Aspects of Metal Phosphine Complexes*, Vol. 196, American Chemical Society, **1982**, pp. 1–22; d) T. G. Appleton, H. C. Clark, L. E. Manzer, *Coord. Chem. Rev.* **1973**, *10*, 335–422; e) W. E. Hill, D. M. A. Minahan, J. G. Taylor, C. A. McAuliffe, *J. Am. Chem. Soc.* **1982**, *104*, 6001–6005.
- [17] F. B. Ogilvie, J. M. Jenkins, J. G. Verkade, *J. Am. Chem. Soc.* **1970**, *92*, 1916–1923.
- [18] a) G. C. Pimentel, A. L. McClellan, *The hydrogen bond*, W. H. Freeman and Co, San Francisco and London, **1960**; b) A. Novak, in *Large Molecules. Structure and Bonding*, Vol. 18, Springer Berlin Heidelberg, Berlin, Heidelberg, **1974**, pp. 177–216; c) G. A. Jeffrey, *An Introduction to Hydrogen Bonding*, Oxford University Press, **1997**; d) T. Steiner, *Angew. Chem.* **2002**, *114*, 50–80; e) T. Steiner, *Angew. Chem. Int. Ed.* **2002**, *41*, 48–76; *Angew. Chem.* **2002**, *114*, 50–80.
- [19] a) G. G. Messmer, E. L. Amma, *Inorg. Chem.* **1966**, *5*, 1775–1781; b) A. N. Caldwell, L. Manojlović-Muir, K. W. Muir, *J. Chem. Soc. Dalton Trans.* **1977**, 2265–2269; c) A. Del Pra, G. Zanotti, *Inorg. Chim. Acta* **1980**, *39*, 137–141; d) G. Robertson, P. Tucker, W. Wickramasinghe, *Aust. J. Chem.* **1986**, *39*, 1495–1507; e) W. M. Attia, G. Balducci, M. Calligaris, *Acta Crystallogr. Sect. C* **1987**, *43*, 1053–1055; f) C. M. DiMeglio, K. J. Ahmed, L. A. Luck, E. E. Weltin, A. L. Rheingold, C. H. Bushweller, *J. Phys. Chem.* **1992**, *96*, 8765–8777; g) H.-K. Fun, S. Chantrapromma, Y.-C. Liu, Z.-F. Chen, H. Liang, *Acta Crystallogr. Sect. E* **2006**, *62*, m1252–m1254; h) J. Chojnacki, A. Robaszekiewicz, E. Matern, E. Baum, J. P. Kikies, *Acta Crystallogr. Sect. E* **2007**, *63*, m680–m682; i) W. Domanska-Babul, J. P. Kikies, J. Chojnacki, *Acta Crystallogr. Sect. E* **2007**, *63*, m2583; j) J. Miao, C. Hu, X. Feng, H. Chen, Y. Nie, *Acta Crystallogr. Sect. E* **2009**, *65*, m1025.
- [20] a) G. Aullón, D. Bellamy, A. Guy Orpen, L. Brammer, E. A. Bruton, *Chem. Commun.* **1998**, 653–654; b) L. Brammer, *Dalton Trans.* **2003**, 3145–3157.
- [21] T. Steiner, *Acta Crystallogr. Sect. B* **1998**, *54*, 456–463.
- [22] S. Suzuki, P. G. Green, R. E. Bumgarner, S. Dasgupta, W. A. Goddard, G. A. Blake, *Science* **1992**, *257*, 942.
- [23] a) M. Levitt, M. F. Perutz, *J. Mol. Biol.* **1988**, *201*, 751–754; b) J. F. Malone, C. M. Murray, M. H. Charlton, R. Docherty, A. J. Lavery, *J. Chem. Soc. Faraday Trans.* **1997**, *93*, 3429–3436; c) T. Steiner, G. Koellner, *J. Mol. Biol.* **2001**, *305*, 535–557; d) G. Desiraju, T. Steiner, *The Weak Hydrogen Bond: In Structural Chemistry and Biology* Oxford University Press, Oxford, **1999**.
- [24] a) K. O. Christe, W. W. Wilson, *J. Fluorine Chem.* **1990**, *47*, 117–120; b) K. O. Christe, W. W. Wilson, R. D. Wilson, R. Bau, J. A. Feng, *J. Am. Chem. Soc.* **1990**, *112*, 7619–7625; c) N. Boechat, J. H. Clark, *J. Chem. Soc. Chem. Commun.* **1993**, 921–922; d) V. V. Grushin, W. J. Marshall, *Organometallics* **2008**, *27*, 4825–4828; e) T. Furuya, J. E. M. N. Klein, T. Ritter, *Synthesis* **2010**, *2010*, 1804–1821; f) S. D. Schimler, S. J. Ryan, D. C. Bland, J. E. Anderson, M. S. Sanford, *J. Org. Chem.* **2015**, *80*, 12137–12145.

- [25] a) R. Laubenstein, M. Ahrens, T. Braun, *Z. Anorg. Allg. Chem.* **2017**, *643*, 1723–1729; b) N. Pfister, T. Braun, P. Wittwer, M. Ahrens, *Z. Anorg. Allg. Chem.* **2018**, *644*, 1064–1070; c) E. Curnock, W. Levason, M. E. Light, S. K. Luthra, G. McRobbie, F. M. Monzittu, G. Reid, R. N. Williams, *Dalton Trans.* **2018**, *47*, 6059–6068; d) P. J. Blower, W. Levason, S. K. Luthra, G. McRobbie, F. M. Monzittu, T. O. Mules, G. Reid, M. N. Subhan, *Dalton Trans.* **2019**, *48*, 6767–6776.
- [26] a) W. W. Wilson, K. O. Christe, J.-a. Feng, R. Bau, *Can. J. Chem.* **1989**, *67*, 1898–1901; b) F. Nahra, S. R. Patrick, D. Bello, M. Brill, A. Obled, D. B. Cordes, A. M. Z. Slawin, D. O'Hagan, S. P. Nolan, *ChemCatChem* **2015**, *7*, 240–244; c) H. C. S. Clark, K. S. Coleman, J. Fawcett, J. H. Holloway, E. G. Hope, J. Langer, I. M. Smith, *J. Fluorine Chem.* **1998**, *91*, 207–211.
- [27] a) K. O. Christe, W. W. Wilson, *J. Fluorine Chem.* **1990**, *46*, 339–342; b) I. G. Shenderovich, S. N. Smirnov, G. S. Denisov, V. A. Gindin, N. S. Golubev, A. Dunger, R. Reibke, S. Kirpekar, O. L. Malkina, H.-H. Limbach, *Ber. Bunsen-Ges. Phys. Chem.* **1998**, *102*, 422–428.
- [28] a) R. Bartsch, O. Stelzer, R. Schmutzler, *Z. Naturforsch. B* **1981**, *36b*, 1349–1355; b) C. B. Caputo, L. J. Hounjet, R. Dobrovetsky, D. W. Stephan, *Science* **2013**, *341*, 1374; c) L. J. Hounjet, C. B. Caputo, D. W. Stephan, *Dalton Trans.* **2013**, *42*, 2629–2635; d) C. B. Caputo, D. Winkelhaus, R. Dobrovetsky, L. J. Hounjet, D. W. Stephan, *Dalton Trans.* **2015**, *44*, 12256–12264.
- [29] a) G. M. Thomas, G. J. Peter, S. Reinhard, *Z. Naturforsch. B* **1993**, *48*, 875–885; b) N. A. Jasim, R. N. Perutz, A. C. Whitwood, T. Braun, J. Izundu, B. Neumann, S. Rothfeld, H.-G. Stammer, *Organometallics* **2004**, *23*, 6140–6149; c) S. A. Macgregor, D. C. Roe, W. J. Marshall, K. M. Bloch, V. I. Bakhmutov, V. V. Grushin, *J. Am. Chem. Soc.* **2005**, *127*, 15304–15321; d) O. Blum, F. Frolow, D. Milstein, *J. Chem. Soc. Chem. Commun.* **1991**, 258–259.
- [30] a) F. H. Allen, A. Pidcock, *J. Chem. Soc. A* **1968**, 2700–2704; b) T. G. Appleton, M. A. Bennett, *Inorg. Chem.* **1978**, *17*, 738–747.
- [31] a) T. Theophanides, P. C. Kong, *Inorg. Chim. Acta* **1971**, *5*, 485–488; b) W. J. Cherwinski, H. C. Clark, *Inorg. Chem.* **1971**, *10*, 2263–2267; c) J. Browning, P. L. Goggin, R. J. Goodfellow, M. G. Norton, A. J. M. Rattray, B. F. Taylor, J. Mink, *J. Chem. Soc. Dalton Trans.* **1977**, 2061–2067; d) C. R. Green, R. J. Angelici, *Inorg. Chem.* **1972**, *11*, 2095–2101; e) G. Vasapollo, C. F. Nobile, A. Sacco, *J. Organomet. Chem.* **1985**, *296*, 435–441.
- [32] a) K. M. Harmon, I. Gennick, *J. Mol. Struct.* **1977**, *38*, 97–107; b) I. Gennick, K. M. Harmon, M. M. Potvin, *Inorg. Chem.* **1977**, *16*, 2033–2040; c) R. R. Lovelace, K. M. Harmon, *J. Mol. Struct.* **1989**, *193*, 247–262; d) K. M. Harmon, R. R. Lovelace, *J. Phys. Chem.* **1982**, *86*, 900–903; e) Y. Shodai, S. Kohara, Y. Ohishi, M. Inaba, A. Tasaka, *J. Phys. Chem. A* **2004**, *108*, 1127–1132.
- [33] a) T. M. Huang, J. T. Chen, G. H. Lee, Y. Wang, *Organometallics* **1991**, *10*, 175–179; b) U. Abram, D. Belli Dell'Amico, F. Calderazzo, L. Marchetti, J. Strähle, *J. Chem. Soc. Dalton Trans.* **1999**, 4093–4098.
- [34] a) B. C. Gorske, C. T. Mbofana, S. J. Miller, *Org. Lett.* **2009**, *11*, 4318–4321; b) O. E. Okoromoba, J. Han, G. B. Hammond, B. Xu, *J. Am. Chem. Soc.* **2014**, *136*, 14381–14384; c) T. J. O'Connor, F. D. Toste, *ACS Catal.* **2018**, *8*, 5947–5951.
- [35] a) G. He, S. Qiu, H. Huang, G. Zhu, D. Zhang, R. Zhang, H. Zhu, *Org. Lett.* **2016**, *18*, 1856–1859; b) G. Zhu, S. Qiu, Y. Xi, Y. Ding, D. Zhang, R. Zhang, G. He, H. Zhu, *Org. Biomol. Chem.* **2016**, *14*, 7746–7753.
- [36] a) K. A. DeKorver, H. Li, A. G. Lohse, R. Hayashi, Z. Lu, Y. Zhang, R. P. Hsung, *Chem. Rev.* **2010**, *110*, 5064–5106; b) G. Evano, A. Coste, K. Jouvin, *Angew. Chem. Int. Ed.* **2010**, *49*, 2840–2859; *Angew. Chem.* **2010**, *122*, 2902–2921; c) C. Madelaine, V. Valerio, N. Maulide, *Chem. Asian J.* **2011**, *6*, 2224–2239; d) X.-N. Wang, H.-S. Yeom, L.-C. Fang, S. He, Z.-X. Ma, B. L. Kedrowski, R. P. Hsung, *Acc. Chem. Res.* **2014**, *47*, 560–578; e) C. Theunissen, B. Métayer, N. Henry, G. Compain, J. Marrot, A. Martin-Mingot, S. Thibaudeau, G. Evano, *J. Am. Chem. Soc.* **2014**, *136*, 12528–12531; f) R. Vanjari, S. Dutta, M. P. Gogoi, V. Gandon, A. K. Sahoo, *Org. Lett.* **2018**, *20*, 8077–8081; g) S. Dutta, S. Yang, R. Vanjari, R. K. Mallick, V. Gandon, A. K. Sahoo, *Angew. Chem. Int. Ed.* **2020**, *59*, 10785–10790; *Angew. Chem.* **2020**, *132*, 10877–10882; h) G. Evano, M. Lecomte, P. Thilmany, C. Theunissen, *Synthesis* **2017**, *49*, 3183–3214; i) A. Lumbroso, J. Behra, A. Kolleth, P.-Y. Dakas, U. Karadeniz, S. Catak, S. Sulzer-Mossé, A. De Mesmaeker, *Tetrahedron Lett.* **2015**, *56*, 6541–6545; j) G. Tanriver, D. Dagoneau, U. Karadeniz, A. Kolleth, A. Lumbroso, S. Sulzer-Mossé, A. De Mesmaeker, S. Catak, *J. Org. Chem.* **2020**, *85*, 449–463.
- [37] I. G. Shenderovich, H.-H. Limbach, S. N. Smirnov, P. M. Tolstoy, G. S. Denisov, N. S. Golubev, *Phys. Chem. Chem. Phys.* **2002**, *4*, 5488–5497.
- [38] a) K. Seppelt, *Angew. Chem. Int. Ed. Engl.* **1992**, *31*, 292–293; *Angew. Chem.* **1992**, *104*, 299–300; b) R. Schwesinger, R. Link, G. Thiele, H. Rotter, D. Honert, H.-H. Limbach, F. Männle, *Angew. Chem. Int. Ed. Engl.* **1991**, *30*, 1372–1375; *Angew. Chem.* **1991**, *103*, 1376–1378; c) R. Z. Gnann, R. I. Wagner, K. O. Christe, R. Bau, G. A. Olah, W. W. Wilson, *J. Am. Chem. Soc.* **1997**, *119*, 112–115.

Manuscript received: July 7, 2021

Accepted manuscript online: August 1, 2021

Version of record online: September 8, 2021